Kinetic Analysis of the Effect on Fab Binding of Identical Substitutions in a Peptide and Its Parent Protein

Laurence Choulier,[‡] Nathalie Rauffer-Bruyère,[‡,§] Myriam Ben Khalifa,[||] Franck Martin,[⊥] Thierry Vernet,[||] and Danièle Altschuh*[,‡]

UPR 9021-CNRS et UPR 9002-CNRS, 15 rue René Descartes, Institut de Biologie Moléculaire et Cellulaire, 67084 Strasbourg Cedex, France, and Laboratoire d'Ingénierie des Macromolécules, Institut de Biologie Structurale, Jean-Pierre Ebel, 41 avenue des Martyrs, 38027 Grenoble Cedex 1, France

Received August 19, 1998; Revised Manuscript Received November 30, 1998

ABSTRACT: Monoclonal antibody 57P, which was raised against tobacco mosaic virus protein, cross-reacts with a peptide corresponding to residues 134−146 of this protein. Previous studies using peptide variants suggested that the peptide in the antibody combining site adopts a helical configuration that mimics the structure in the protein. In this study, we carried out a detailed comparison of Fab−peptide and Fab−protein interactions. The same five amino acid substitutions were introduced in the peptide (residues 134−151) and the parent protein, and the effect of these substitutions on antibody binding parameters have been measured with a Biacore instrument. Fabs that recognize epitopes located away from the site of mutations were used as indirect probes for the conformational integrity of protein antigens. Their interaction kinetics with all proteins were similar, suggesting that the substitutions had no drastic effect on their conformation. The five substitutions introduced in the peptide and the protein had minor effects on association rate constants (k_a) and significant effects on dissociation rate constants (k_d) of the antigen−Fab 57P interactions. In four out of five cases, the effect on binding affinity of the substitutions was identical when the epitope was presented in the form of a peptide or a protein antigen, indicating that antibody binding specifity was not affected by epitope presentation. However, k_a values were about 10 times larger and k_d values about 5 times larger for the peptide−Fab compared to the protein−Fab interaction, suggesting a different binding mechanism. Circular dichroism measurements performed for three of the peptides showed that they were mainly lacking structure in solution. Differences in conformational properties of the peptide and protein antigens in solution and/or in the paratope could explain differences in binding kinetics. Our results demonstrate that the peptides were able to mimic correctly some but not all properties of the protein−Fab 57P interaction and highlight the importance of quantitative analysis of both equilibrium and kinetic binding parameters in the design of synthetic vaccines and drugs.

Cross-reactivity is an intriguing aspect of immune recognition that has been extensively studied and discussed (*1*−*3*). Peptides able to cross-react with antibodies raised against the parent protein have been used to map epitopes (*4*−*8*). Anti-peptide antibodies that are able to cross-react with the parent protein are useful probes for detecting the protein in complex cellular extracts and may also be relevant in the design of synthetic vaccines (*9*−*11*).

The structural basis of cross-reactivity can be analyzed by comparing the conformations of the free and bound peptide with those of the free and bound protein antigen. However, such a complete data set is not yet available. So far, structural studies by X-ray crystallography and NMR have addressed two features important for immune cross-reactivity. The first is the degree of structural similarity present between a peptide bound in the antibody combining site and the same sequence in the folded protein. In some systems no overall similarity was found (*12*−*15*), while in others a partial structural similarity was observed (*16*−*19*). These examples include antibodies raised to viruses, proteins, and peptides. The second issue is the degree of conformational similarity between free and bound antigens. Structural differences between free and bound protein antigens were found to be barely significant (*20*−*24*). The situation was different for peptides that are flexible in solution or present in a number of different conformational states (*25*, *26*). Peptides that were structured in solution (*27*−*29*) were found to adopt different conformations when bound to different antibodies (*17*, *30*, *31*). Furthermore, NMR studies indicated that peptides may retain considerable mobility when bound to the antibody (*32*).

The functional consequences of differences in structural properties between peptides and proteins have rarely been studied in detail, although it has been shown that the affinity of an antibody for a protein and a peptide analogue may differ by one or more logarithmic units. Differences in the binding kinetics of two antigenic forms have been reported for example in the human immunodeficiency virus 1 system (*33*) and the tryptophan synthase system (*34*).

* To whom correspondence should be addressed: Phone: (33) 3 88 41 70 24; Fax (33) 3 88 61 06 80; E-mail alt@ibmc.u-strasbg.fr.
[‡] UPR 9021-CNRS, Institut de Biologie Moléculaire et Cellulaire.
[§] Present address: Plant Molecular Biology Center, Northern Illinois University, De Kalb, IL60115-2861, USA.
[||] Institut de Biologie Structurale, Jean-Pierre Ebel.
[⊥] UPR 9002-CNRS, Institut de Biologie Moléculaire et Cellulaire.

10.1021/bi982011z CCC: $18.00
Published on Web 03/05/1999

In the present study, we analyze two aspects of the binding of a peptide and its parent protein to an antibody. The first aspect is binding kinetics, since on and off rates determine the process of molecular recognition. Kinetics are likely to be essential for efficient biological activity in vivo, where interactions generally occur between a number of competing molecules. The importance of kinetics in the immune system has been discussed (*35*, *36*). The second aspect is the effect that the same amino acid substitutions, introduced in the peptide and protein antigens, have on kinetic rate constants and binding affinity. The ability of an antibody to discriminate between a range of antigenic variants is a measure of binding specificity. Specificity of binding is required for any application using peptide analogues.

The strategy was to introduce the same amino acid substitutions in the peptide and in the protein and to measure the effect of these changes on interaction kinetics with a Biacore instrument (Biacore AB, Uppsala, Sweden). Biacore is a biosensor based on surface plasmon resonance that allows molecular interactions to be followed in real time. For simple interaction systems, analysis of the interaction curves yields association (k_a)[1] and dissociation (k_d) rate constants, from which the equilibrium constant (K_a) can be calculated.

Earlier studies have established that monoclonal antibody 57P, raised against tobacco mosaic virus protein (TMVP), cross-reacts with a peptide corresponding to residues 134−146 of this protein (*37*). In the crystal structure of TMVP, residues 141−148 form a short α-helix (*38*, *39*). The interaction of antibody 57P with a set of 15 peptide variants carrying single residue substitutions has been analyzed with Biacore. The recognition pattern suggested that the peptide in the antibody combining site adopts a helical configuration that mimics the structure in the protein (*6*). In the present study, we compare the effect of five identical substitutions in the recombinant viral protein and in a synthetic peptide (residues 134−151) on binding to recombinant Fab 57P (*40*), and the related Fab 145P (M. Ben Khalifa, manuscript in preparation). In four out of five cases, the effect on binding affinity of the substitutions was identical when the epitope was presented in the form of a peptide or a protein antigen, indicating that antibody specifity was not affected by epitope presentation. However, the kinetics of binding were significantly different for the two antigenic forms, suggesting a different mechanism of binding.

EXPERIMENTAL PROCEDURES

Fab Fragments. Monoclonal antibodies (mAb) 57P, 121P, and 270P were elicited against TMVP (*41*). Antigen binding fragments (Fab) derived from mAbs 121P and 270P were obtained and purified as described (*42*). The Fab of mAb 57P has been cloned and expressed in *Escherichia coli* (*40*). Fab 145P differs from Fab 57P by four amino acid changes: $G^{L26}S$, $L^{L37}F$, $L^{L38}Q$, and $Y^{H91}F$ (M. Ben Khalifa, manuscript in preparation).

Synthetic Peptides. Peptides were prepared by solid-phase peptide synthesis using standard Fmoc chemistry. Peptide C-WT corresponds to residues 134−151 of TMVP, with an additional N-terminal cysteine to allow chemical coupling to CM5 sensor chips. The following substituted peptides derived from this wild-type sequence were used: C-S142E, C-S142N, C-E145A (*43*), C-S142A, and C-S146A.

Circular Dichroism. Circular dichroism (CD) spectra were recorded in the far ultraviolet (190−250 nm) with a dichrograph model CD6 (Jobin Yvon, France). The instrument was routinely calibrated with an aqueous solution of d-10-camphorsulfonic acid. Quartz cells of 0.1 cm were used and the data were collected at 0.5 nm intervals; 5 s time constant. Samples were kept at 22 °C (± 1 °C) by a circulating water bath. All the spectra were the average of series of five scans. Buffer blanks were subtracted from the corresponding samples. Peptide concentrations ranging from 0.43 to 0.52 mg/mL in 20 mM sodium phosphate buffer, pH 7.5, were used. When necessary a final concentration of 50% trifluoroethanol (TFE) was added. Molar ellipticity [θ] is expressed in degrees·cm^2·dmol^{-1} and derives from $[\theta] = (\theta_{obs})(100/lc)$, where θ_{obs} is the observed ellipticity, l is the light path length (in centimeters), and c is the peptide concentration in moles per liter of chromophore.

Mutagenesis of Recombinant Protein Antigens. The vector pET3a carrying the sequence of TMVP (*44*) is a kind gift from Professor T. M. A. Wilson (Scottish Crop Research Institute, Dundee, U.K.). A six-histidine extension was added C-terminal to TMVP by overlapping polymerase chain reaction (PCR) to allow purification of the recombinant proteins by affinity chromatography on a nickel matrix (*45*). The tendency of TMVP to aggregate leads to unstable baseline levels on BIAcore due to the leaking of protein subunits during surface regeneration, and to heterogeneous interaction kinetics. Mutations T28I and E95D were introduced by PCR in TMVP because the chemical mutant PM2 carrying these changes has been shown to display reduced aggregation properties (*46*). This modified protein, thereafter referred to as CPmutHis, still aggregates but to a lesser extent than the wild-type protein, and its interaction kinetics with Fab 57P are homogeneous.

The mutations in the gene coding for the protein CPmutHIS were created by site-directed mutagenesis (*47*) using single-strand DNA from the vector pET23a (Novagen) carrying the sequence of CPmutHis as template and mutagenic oligonucleotides (Table 1). The single-stranded DNA and its mutant derivatives were prepared by using strain CJ236 (F′cat(=pCJ105; M13^s Cm^r)/*dut ung thi*-1 *relA1 spoT1 mcrA*) as cellular host and M13K07 as helper phage (*48*).

The DNA molecules synthesized in vitro were introduced into strain BL21 (F^- *ompT* r_B^- m_B^-) (*49*) for their amplification and were extracted by alkaline lysis (*50*). The presence of mutations was checked by restriction analysis (Table 1) and confirmed by DNA sequencing (Genome Express, Grenoble, France).

Expression and Purification of Protein Antigens. Wild-type and mutant proteins were expressed in strain BL21-(DE3)pLysE, which contains the plasmid pLysE coding for chloramphenicol resistance and for phage T7 lysozyme (*49*), allowing tight regulation of gene expression. A preculture

[1] Abbreviations: CD, circular dichroism; EDC, *N*-ethyl-*N*′-[3-(diethylamino)propyl]carbodiimide; EDTA, ethylenediaminetetraacetic acid; ELISA, enzyme-linked immunosorbent assay; Fab, fragment antigen binding; HEPES, *N*-(2-hydroxyethyl)piperazine-*N*′-2-ethanesulfonic acid; IPTG, isopropyl β-D-thiogalactopyranoside; k_a, association rate constant; k_d, dissociation rate constant; K_a, equilibrium association constant; mAb, monoclonal antibody; NHS, *N*-hydroxysuccinimide; NTA, trinitriloacetic acid; PCR, polymerase chain reaction; RU, resonance units; SDS, sodium dodecyl sulfate; TFE, trifluoroethanol; TMVP, tobacco mosaic virus protein.

Table 1: Sequence of Oligonucleotides Used for Site-Directed Mutagenesis[a]

Mutants	Oligonucleotides	Diagnostic
S142A	5'-CCAGAAGAGCTCTCGAA**GCTAGC**CCGATTATAAGATCCGG-3'	*Nhe I*
S142E	5'-GAAGAGCTCTCGAAAGA**TTCGCGA**TTATAAGATCCGG-3'	*Nru I*
S142N	5'-CAAACCAGAAGAGCT**TTCGAA**AGAG**T**TCCGATTATAAGATCC-3'	*Bst BI*
E145A	5'-CCAGAAGA**GCTAGC**GAAAGAGCTCC-3'	*Nhe I*
S146A	5'-CCAAACCAAACCAGA**GCTAGC**CTCGAAAGAGCTCCG-3'	*Nhe I*

[a] Mutated oligocleotides are shown in boldface type; Restriction sites are underlined.

was grown overnight at 37 °C in Luria−Bertani medium (*50*) supplemented with 100 mg/mL ampicillin and 17 mg/mL chloramphenicol. A volume of 250 μL of this preculture was added to 50 mL of fresh medium and incubated at 37 °C until an $OD_{600nm} = 0.6-1$ was reached. Protein expression was then induced by 0.4 mM isopropyl β-D-thiogalactopyranoside (IPTG) at 25 °C overnight. The bacteria were harvested by a 4000 rpm centrifugation at 4 °C. The pellet was resuspended in 10 mL of a sonication buffer (50 mM $Na_2HPO_4 \cdot 2H_2O$ and 300 mM NaCl, pH 7.8), frozen, and thawed to lyse the bacteria. The lysate was further disrupted by a 1 min sonication at 120 V and 4 °C. The cell soluble fraction was recovered from the supernatant of a 15 min centrifugation at 9000 rpm.

Five milliliters of the soluble fraction was loaded onto a 250 mL Ni−NTA column (Qiagen) equilibrated in the sonication buffer. After 1 h of contact on ice, the column was centrifuged at 2000 rpm for 5 min. The supernatant was removed, the column was washed twice with 2 mL of washing buffer (50 mM $Na_2HPO_4 \cdot 2H_2O$, 300 mM NaCl, and 10% glycerol, pH 6.0), left on ice 10 min, and centrifuged again. The proteins were then eluted twice with 1 mL of washing buffer containing 100 mM imidazole and dialyzed against HEPES buffer (1 mM HEPES, pH 7.4, 340 μM EDTA, and 15 mM NaCl) at 4 °C overnight.

The purity of the proteins was checked by electrophoresis on SDS−12.5% polyacrylamide gels, stained with Coomassie blue. Western blots (*51*) were performed with an anti-TMVP polyclonal antibody as primary antibody and goat anti-rabbit immunoglobulin conjugated either to alkaline phosphatase (Sigma) or to peroxidase (Sigma) for detection.

Preparation of Sensor Surfaces. Immobilization of antigens to sensor surfaces was performed as described previously (*52*; BIAapplications Handbook, Biacore, Uppsala, Sweden).

Briefly, peptides at a concentration of 50 μg/mL in 10 mM formic acid, pH 3.2, were immobilized on the carboxylated dextran matrix of CM5 sensor chips through the sulfhydryl group of the N-terminal Cys (*43*) by thiol activation chemistry. Control surfaces were obtained by treating the surface as for peptide immobilization, except that peptide injection was omitted.

Proteins were immobilized on CM5 sensor chips through their primary amine groups. The matrix was activated with 50 μL of a solution containing *N*-ethyl-*N*′-[3-(diethylamino)-propyl]carbodiimide (EDC) and *N*-hydroxysuccinimide (NHS). In view of its low p*I* (4.5), TMVP was injected at a concentration of 5 μg/mL in 10 mM formic acid at pH 3.5. The immobilization procedure was completed by a 5 min injection of 1 M ethanolamine hydrochloride to block remaining ester groups. The washing and regeneration steps were done by successive injections of 50 mM HCl. Blank surfaces were obtained by treating the surface as for protein immobilization, except that protein injection was omitted.

Determination of Fab Concentrations. The concentration of active Fab 57P was determined with BIAcore by varying the flow rate under conditions of partial mass transport limitation (*42*, *53*). This method allows the precise determination of active Fab concentrations without the need of a calibration curve. The time required for this experiment is about 1 h, and Fab concentration must be adjusted to 10 ± 5 nM. Fab 57P was injected during 2−5 min on a surface containing high concentrations of peptide, at flow rates ranging from 2 to 100 μL/min. Binding curves were analyzed by the BIAconc program (*53*) available on the worldwide web (http://www.be.dtu.dk/~lc/).

After its concentration had been determined in this way, the Fab preparation was used to establish a calibration curve, which will subsequently allow the rapid (10 min) determination of Fab concentration in all solutions (concentrations ranging from 5 to 100 nM) prepared for kinetic runs. Surfaces contained high concentrations of peptide, so that the binding rates were limited by mass transport and independent of affinity (*54*). Aliquots (10 μL) of Fab solutions at concentrations ranging from 5 to 100 nM were injected at a flow rate of 10 μL/min, and the binding rate measured 10 s after injection was plotted against Fab concentration. By use of this calibration curve, Fab concentrations in each solution used for kinetic measurements were determined immediately before the kinetic run. This procedure was used to minimize errors due to pipetting and/or partial inactivation of Fab either during storage in the freezer or in the Biacore rack and was crucial for obtaining reproducible k_a values.

Kinetic Measurements. The kinetics of interaction between the different Fabs and the immobilized antigens were followed with a BIAcore2000 instrument. Fabs at concentrations of approximately 72, 24, and 8 nM (calibrated before each kinetic run) were injected in 10 mM HBS buffer at a constant flow of 10 μL/min at 25 °C. Surface immobilization levels were adjusted in order to bind a maximum of 500−600 RU of Fab in saturating conditions. Antigen surfaces were regenerated by injecting 10 μL of 50 mM HCl.

Kinetic data were interpreted with the BIAevaluation 2.1 or 3.0 software (Biacore, Uppsala, Sweden). For a simple 1:1 model of interaction between two molecular species, the exponential function that describes the response (R_t) in

resonance units as a function of time (t) during the post-injection phase is

$$R_t = R_0 \, e^{-k_d(t-t_0)}$$

where R_0 and t_0 are the values of R_t and t, respectively, at the start of the time range for measurements and k_d is the dissociation rate constant. For the injection phase, the equation is

$$R_t = R_{eq} \, [1 - e^{-(k_a C + k_d)(t-t_0)}]$$

where R_{eq} is the response at equilibrium, C is the molar concentration of Fab, t_0 is the value of t at the start of measurements, and k_a is the association rate constant.

In early experiments, kinetic data were analyzed by the nonlinear least-squares method (*55*), using the BIAevaluation 2.1 software. Subsequently data were analyzed with algorithms for numerical integration and global analysis (*56*) using the BIAevaluation 3.0 software (*57*).

The dextran matrix is neither a solid phase nor a liquid phase but may be approximated by a semiliquid phase (*54*). The apparent equilibrium association constant K'_a for the interaction between the Fab and an antigen covalently attached to the dextran is given by

$$K'_a = k_a/k_d$$

and the effect of substitutions on the binding energy is given by

$$\Delta\Delta G = -RT \ln (K'_{a\,mut}/K'_{a\,WT})$$

where R is the universal gas constant, T is the temperature (298 K), and $K'_{a\,mut}$ and $K'_{a\,WT}$ are the apparent equilibrium affinity constants for mutant and wild-type antigen, respectively.

RESULTS

Mutagenesis and Expression of Protein Antigens. The epitope recognized by mAb 57P has been mapped previously with variants of peptide 134−146 of TMVP (*6*). In the present study, we chose to modify positions 142, 143, and 145, which had been shown to contribute to antigen binding, as well as position 146, which is adjacent to positions 142 and 143 in the folded protein. The following substitutions were selected for site-directed mutagenesis: S142A, S142E, S142N, S143A, E145A, E145D, E145Q, S146A, and S146D, as well as the double change S142E−E145A. The proteins were expressed in bacterial strain BL21pLysE (DE3).

Six of the mutant proteins (S143A, E145Q, E145D, E145S, S146D, and S142E−E145A) were expressed in amounts insufficient for functional analysis. Experiments were therefore conducted with the five proteins S142A, S142E, S142N, E145A, and S146A. The purified proteins were obtained at a concentration of 0.1−0.6 mg/mL (as measured by the OD at 280 nm), and their binding properties were compared with those of the corresponding peptide antigens.

Interaction of Protein Variants with Fabs Recognizing Regions Outside the Sites of Mutation. mAbs 121P and 270P, directed against regions 115−134 and 76−88 of TMVP, respectively, were used to evaluate the conformational integrity of mutant proteins. These antibodies recognize conformational epitopes since they interact with the protein in an ELISA double antibody sandwich assay, in which the protein is presented by a first polyclonal antibody and is presumably folded (*58*). They are also able to inhibit in vitro cotranslational disassembly of tobacco mosaic virus (*59*). Different concentrations of Fabs 121P and 270P were injected on surfaces immobilized with proteins CPmutHIS, S142E, S142N, E145A, and S146A. No antigen was injected during the postinjection phase. Kinetic constants for the interaction between the Fabs and the proteins were evaluated by the BIAevaluation 2.1 software (Biacore, Uppsala, Sweden), and are presented in Figure 1. The calculated values are similar for all proteins, suggesting that the mutations introduced in the proteins did not greatly affect their conformation.

Conformation of the Free Peptides As Evaluated by Circular Dichroism. Circular dichroism spectra were recorded for C-WT, C-S142E, and C-E145A peptides in an attempt to evaluate and compare their propensity for secondary structure formation in solution. The spectra show a minimum molar ellipticity at 198−201 nm in aqueous buffer, which is characteristic of a random structure (Figure 2a). The characteristic signature minima of α-helix at 208 and 222 nm were not detected in those conditions. Since the peptide epitope has an α-helical conformation in TMVP we have recorded CD spectra of each peptide in the presence of 50% TFE, a α-helix-promoting organic compound (*60*). Addition of TFE decreased the ellipticity at 200 nm for all three peptides and increased the magnitude of the ellipticity at 222 nm for the C-S142E and C-E145A peptides (Figure 2b). These changes indicate a modest but significant decrease in random structures concomitant with an increase in the propensity of α-helical conformation.

Quality of Kinetic Data Using Fabs 57P and 145P. The rate constants for the interaction between Fabs 57P and 145P (specific for the mutated region) and the different antigens were analyzed by the global fitting algorithm of the BIAevaluation 3.0 software package. Between two and five independent measurements on different surfaces were performed for each antigen−Fab pair. The values of the rate constant represent the mean that was calculated after rejecting values that differed by more than 1 standard deviation from the overall mean. In these experiments, values that were rejected represented 17% of all data. Standard deviations on k_a and k_d were less than 15% for peptide interactions and less than 20% for protein interactions. The χ^2 values were always below 10, indicating that the simple 1:1 model of interaction correctly described the experimental data. An example of typical data for the interaction between protein S142E and corresponding peptide C-S142E with Fab 57P is given in Table 2.

Interaction of Mutant Antigens with Fabs 57P and 145P. Fab 145P showed a comparable association rate and faster dissociation rate compared to Fab 57P, but the patterns of antigen recognition were similar for the two Fabs. Figure 3 illustrates k_a and k_d values calculated with the two Fabs using the protein antigens. This consistency of data obtained with two related Fabs demonstrates the reliability of even small differences in measured kinetic rates. However, because the data obtained with Fab 57P always had smaller error bars, data will be discussed below with respect to Fab 57P only.

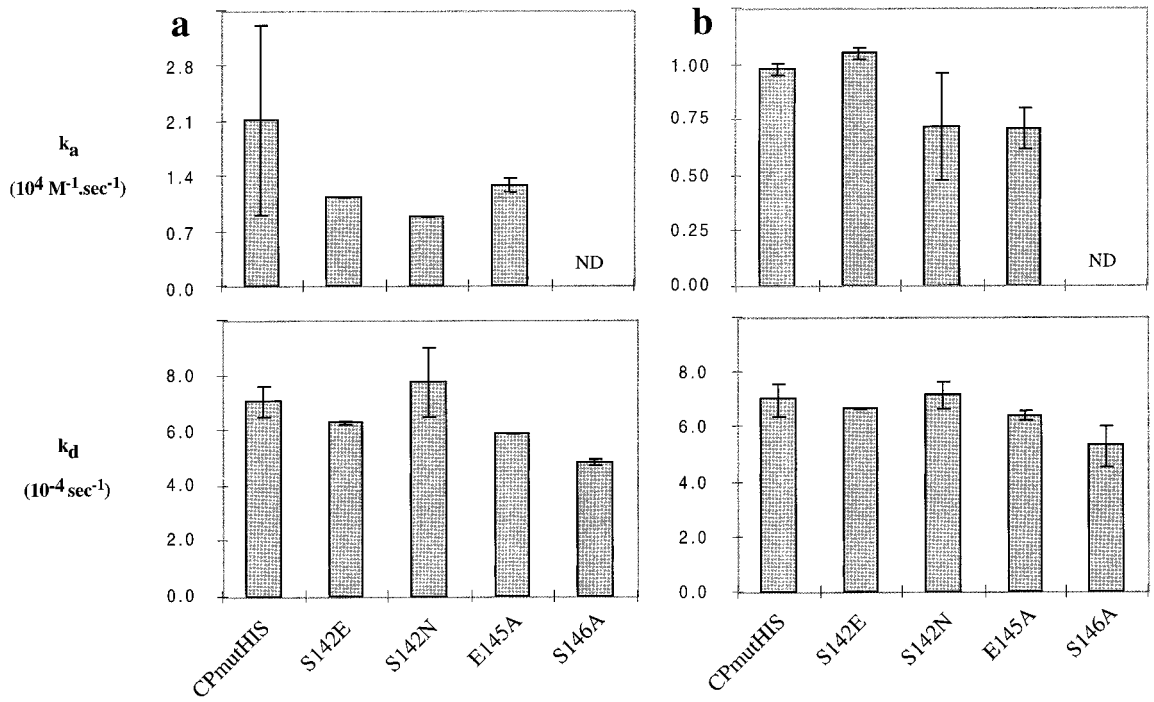

FIGURE 1: Effect of four substitutions in the proteins on kinetic rates for their interaction with Fabs 121P (a) and 270P (b) directed to regions l15−134 and 76−88 of TMVP, respectively. ND, not determined.

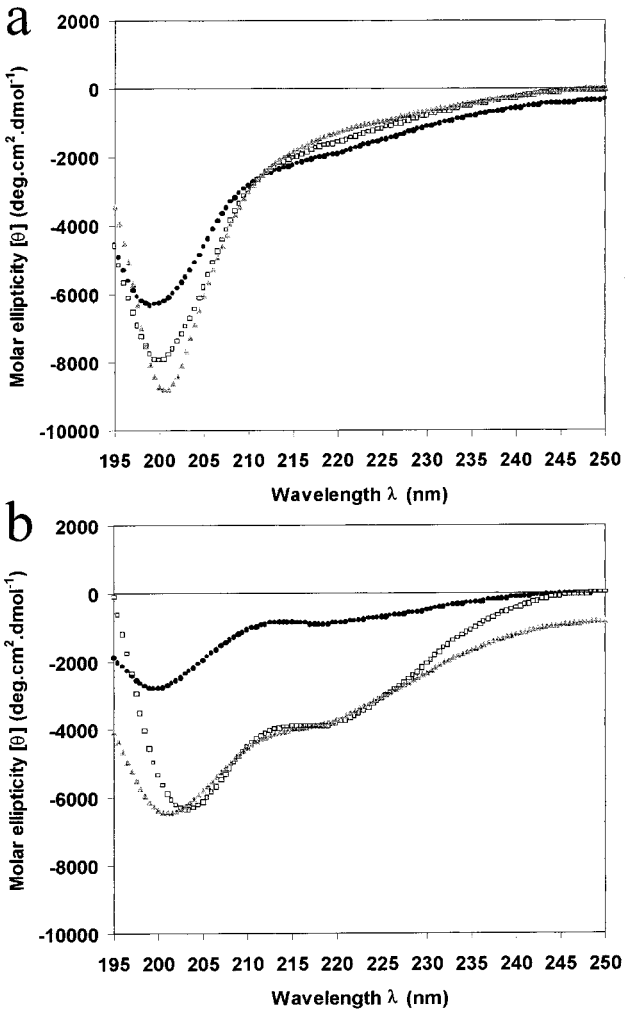

FIGURE 2: Circular dichroism spectra of three peptides in absence of TFE (a) and with 50% TFE (b). (●) Peptide C-WT; (□) peptide C-S142E; (▲) peptide C-E145A.

Rate constants obtained for the interaction between the peptide and protein antigens with Fab 57P are shown in Figure 4. Two observations can be made: the patterns of rate constant variations as a function of the mutation are superimposable for peptide and protein antigens (compare the patterns in Figure 4 panels a and b for k_a and in Figure 4 panels c and d for k_d). One exception is the different effect of mutation E145A on k_d of the Fab−protein and Fab−peptide interactions. The second observation is that the rate constants for protein and peptide interactions are significantly different. The peptides consistently associated and dissociated faster than the proteins (compare the scales in Figure 4 panels a and b for k_a and in Figure 4 panels c and d for k_d).

DISCUSSION

Relative Effect of Mutations on Kinetic Rates. The different mutations had only minor effects on association rate constants. The ranking of k_a values was nearly superimposable for the interaction of the mutated proteins and peptides (Figure 4a,b) with Fab 57P, suggesting that even the smallest differences may be real, although only the 40% decrease in k_a observed with substitution S142E is significant when error bars are considered. Substitutions had significant effects on dissociation rates. The ranking of k_d values was the same for the peptide and the protein antigens in four out of five cases: S142A, S142E, S142N, and S146A (Figure 4c,d). The observed similarity in recognition patterns indicates that the peptides are able to mimic fine details of the binding properties of the protein antigens.

There is, however, one exception to the similarity in effects, showing that no general rule applies. Mutation E145A increased k_d for the peptide−Fab interaction ($k_{d\,E145A}/k_{d\,WT} = 7.4$) but had no effect on Fab−protein dissociation ($k_{d\,E145A}/k_{d\,WT} = 1.1$). The side chain of residue 145 may form a contact with the paratope in the peptide−Fab complex but not in the protein−Fab complex. Alternatively, removal of

Table 2: Binding Parameters Calculated for the Interaction between Fab 57P and Antigens with Substitution S142E in Four Independent Experiments, and Overall Mean

antigens	expt	k_a (10^4 $M^{-1}.s^{-1}$)	k_d (10^{-3} s^{-1})	K_a (10^7 M^{-1})	χ^2 [a]
S142E (protein)	1	4.09 ± 0.03	3.02 ± 0.01	1.35	0.74
	2	4.98 ± 0.02	2.41 ± 0.01	2.07	1.12
	3	*2.62*[b] *± 0.05*	2.75 ± 0.02	*0.95*[b]	8.22
	4	4.84 ± 0.02	2.33 ± 0.01	2.08	0.35
	mean	4.64 ± 0.48	2.63 ± 0.32	1.83 ± 0.42	
C-S142E (peptide)	1	38.5 ± 0.86	12.9 ± 0.12	2.98	3.14
	2	*29.0*[b] *± 0.34*	*4.8*[b] *± 0.04*	*6.00*[b]	3.6
	3	44.8 ± 0.28	11.4 ± 0.03	3.91	3.14
	4	42.1 ± 0.25	10.4 ± 0.03	4.05	6.63
	mean	41.8 ± 3.16	11.6 ± 1.26	3.65 ± 0.58	

[a] The χ^2 values are those given by the BIAevaluation 3.0 software. [b] Values in italic type have been excluded to calculate the mean.

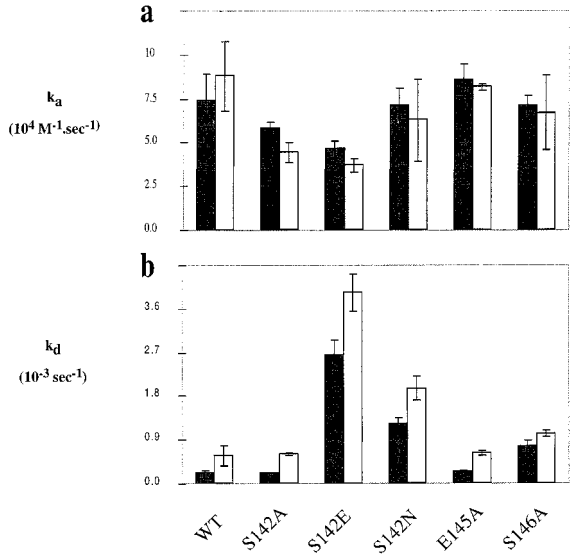

FIGURE 3: Comparison of the effect of substitutions in the protein antigens on k_a (a) and k_d (b) of their interaction with Fab 57P (dark gray) and 145P (light gray). WT refers to protein CPmutHis.

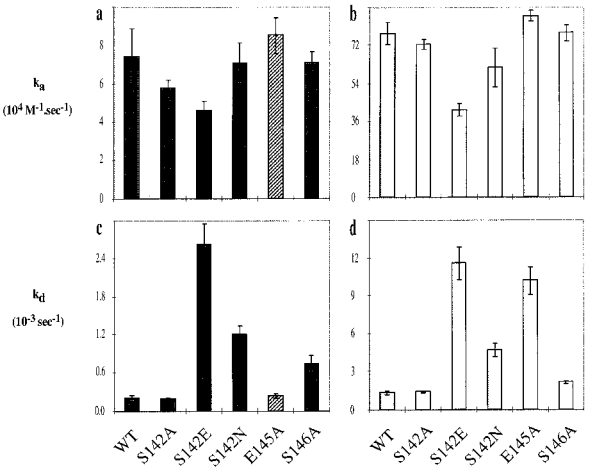

FIGURE 4: Comparison of the effect on k_a (panels a and b) and k_d (panels c and d) of identical substitutions in the protein (dark gray; panels a and c) and peptide (light gray; panels b and d) antigens for their interaction with Fab 57P. Data obtained with antigens carrying the substitution E145A, which had a different effect on k_d in the peptide and protein, are shown by hatched bars.

the E145 side chain may affect peptide recognition by modifying its conformational properties. In particular, the E145 side chain may help stabilize a conformation of the wild-type peptide that is favorable to antibody binding.

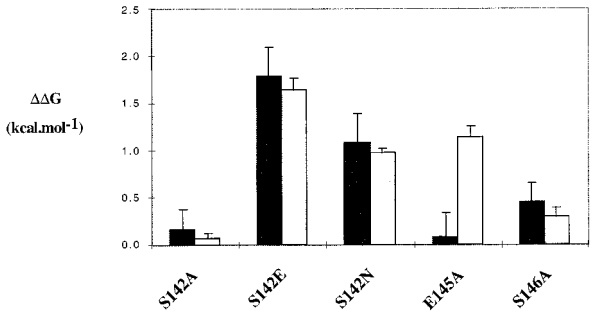

FIGURE 5: Comparison of the effect on binding energy of identical changes in the protein (dark gray) and peptide (light gray) antigens on interaction with Fab 57P. The $\Delta\Delta G$ is calculated as $\Delta G_{mut} - \Delta G_{WT}$. Data obtained with antigens carrying the substitution E145A, which had a different effect on k_d in the peptide and protein, are shown by hatched bars.

Effect on Binding Energy of Substitutions. The equilibrium affinity constant calculated with the Biacore may be considered as an apparent rather than absolute value (*8*), because one of the interactants is covalently attached to the dextran matrix of a sensor chip. However, differences in K'_a values measured in identical experimental conditions are reliable and can be used to calculate the effect on binding energy of amino acid changes in the two antigenic forms.

The energetic consequences of the four mutations S142A, S142E, S142N, and S146A are identical when the epitope is presented in the form of a peptide or protein (Figure 5). The reproducibility of values obtained for four of the five mutants indicates that the ability of the antibody to discriminate between antigenic variants is independent of the type of antigen used for mutational analysis. Similar results were obtained with an antibody to myohemerythrin in a semiquantitative assay (*61*) and recently with an antibody to the TrpB2 subunit of tryptophan synthase with a quantitative ELISA competiton assay (*62*).

Since the structure of the antigen−Fab complex is not known, there is no information on the atomic environment of Ser 142 and 146 at the epitope/paratope interface. However, two of the four changes correspond to the removal of a Ser side chain (S142A and S146A). The energetic consequence of this change, which should reflect the apparent contribution of the serine hydroxyl to complex stability, is insignificant in both cases, suggesting that the two Ser side chains do not form productive bonds at the paratope/epitope interface. In contrast, removal of the hydroxyl of Ser143, which is adjacent to Ser142 and Ser146 in the folded protein, decreased the binding affinity below a detectable level (*6*).

The 1.7 and 1.0 kcal/mol variation in ΔG observed when Ser142 is replaced by Glu or Asn, respectively, may reflect steric hindrance due to the introduction of a larger side chain at the paratope/epitope interface. The reproducibility of the effect of these changes in the peptide and protein antigens would imply that the new side chains are accommodated in the same way in both complexes. Alternatively, the effect of these changes may reflect an altered stability of the free antigens.

Our study and that of Rondard and Bedouelle (*62*) indicate that alternative antigenic forms may be advantageously used to evaluate binding specificity of an antibody raised to a protein. This may be a general rule when the peptide is recognized in a conformation that mimics the native protein. The alternative antigenic forms were synthetic peptides (this study) and a recombinant hybrid protein (*62*), because of their ease of production, purification, and modification.

Differences in Kinetic Rates for Protein and Peptide Antigens. Kinetic rate constants of the peptide−Fab and protein−Fab interactions are significantly different (Figure 4). For the four mutants showing a similar ranking of peptide recognition (S142A, S142E, S142N, and S146A), k_a values are about 10 times larger for the peptide compared to the protein antigens (8.7−12.5 depending on the mutant), and k_d values are about 5 times larger (2.9−6.9 depending on the mutant). The faster kinetic rates of peptide compared to protein interactions may not be explained by the greater diffusion coefficient of a small peptide compared to a protein. In the assay format used, the peptide and protein antigens are attached to the dextran matrix, and it is the Fab that is injected in the flow in all interactions studied. The apparent equilibrium affinity values K'_a are on average 1.8 times larger for the protein−Fab interactions, compared to the peptide−Fab interactions (1.5−2.0 depending on the mutant). The only 2-fold difference in apparent equilibrium affinity values suggests that atomic bonds that are formed at the paratope/epitope interface are similar in the Fab−peptide and Fab−protein complexes, unless differences in the forces contributing to complex stability cancel out.

Different mechanisms of molecular recognition have been proposed. Burgen et al. (*63*), in particular, proposed a relationship between binding mechanism and interaction kinetics, which could explain the faster interaction kinetics of the peptides compared to the proteins that we observe here. They consider two contrasting models for the binding mechanism. The first is an extension of the lock and key model in which a molecule must be presented in a correct conformation and orientation for forming a stable complex. The second is the zipper model, where a nucleation complex is initially formed between the two molecules, followed by a series of conformational rearrangements of the partly bound ligand, leading to binding of the remaining segments to their appropriate subsites. According to Burgen et al. (*63*), the association rate is determined by the nucleation step in the zipper model and should be rapid compared to that in the first model. If the final state is the same in both models of interaction, then equilibrium affinity should be the same even though the pathways of complex formation are different. A higher association rate in the zipper, compared to the lock and key model, should be compensated by a higher dissociation rate.

CD spectra showed that the wild-type peptides and two of the mutant peptides (C-S142E and C-E145A) were mainly lacking structure in solution. A small population of the mutant peptides might be present as an α-helix in aqueous buffer since the addition of TFE slightly increases the proportion of α-helix (Figure 2b). This effect was much less marked with the wild-type peptide. Some flexibility of the peptides in solution and/or in the antibody combining site could explain the faster association and dissociation of the Fab−peptide interactions compared to the protein−Fab interactions. The Fab could bind the peptide rapidly according to the zipper model, while orientational and conformational restrictions of the protein antigen, particularly when attached to the dextran matrix of a sensor chip, may slow recognition. As predicted by the theory, dissociation of the peptides from the paratope is also faster than dissociation of the proteins. If transient complexes with various stabilities are present during the time scale of a Biacore experiment, this mechanism should lead to heterogeneous binding kinetics, which were not observed. Formation of the final peptide−Fab complex after the initial nucleation step is therefore expected to be a fast process. The data also suggest that a large fraction of the peptide is present in a conformation that allows nucleation within the time frame of the Biacore experiment.

CONCLUSION

Our study demonstrates that the peptides were able to mimic correctly some but not all binding properties of protein antigens. Antibody binding kinetics differed significantly, although apparent equilibrium affinity values were close and although the energetic effects of four out of five substitutions were the same when introduced in the peptide and protein antigens. These observations highlight the importance of a quantitative analysis of both equilibrium binding and kinetic parameters in the design of efficient vaccines, and in general of inhibitors or other drugs (*64*, *65*).

ACKNOWLEDGMENT

We thank Dr. M. H. V. Van Regenmortel for stimulating discussion and constant support, Professor T. M. A. Wilson (Dundee, U.K.) for the kind gift of the TMVP clone, Drs. Gilbert Eriani and Jean Gangloff for help and advice in protein engineering, and Drs. J.-P. Briand and J.-P. Roussel for peptide synthesis.

REFERENCES

1. Lerner, R. A. (1984) *Adv. Immunol. 36*, 1−44.
2. Roberts, V. A., Getzoff, E. D., and Tainer, J. A. (1993) in *Structure of antigens* II (Van Regenmortel, M. H. V., Ed.) pp 31−53, Telford and CRC Press, Boca Raton, FL.
3. Van Regenmortel, M. H. V. (1999) *J. Immunol. Methods* (in press).
4. Geysen, H. M., Rodda, S. J., Mason, T. J., Tribbick, G., and Schoofs, P. G. (1987) *J. Immunol. Methods 102*, 259−274.
5. Getzoff, E. D., Geysen, H. M., Rodda, S. J., Alexander, H., Tainer, J. A., and Lerner, R. A. (1987) *Science 235*, 1191−1196.
6. Altschuh, D., Dubs, M. C., Weiss, E., Zeder-Lutz, G., and Van Regenmortel, M. H. V. (1992) *Biochemistry 31*, 6298−6304.

7. Volkmer-Engert, R., Ehrhard, B., Hellwig, J., Kramer, A., Höhne, W., and Schneider-Mergener, J. (1994) *Lett. Pept. Sci. 1*, 243−253.
8. Rondard, P., Goldberg, M. E., and Bedouelle, H. (1997) *Biochemistry 36*, 8962−8968.
9. Getzoff, E. D., Tainer, J. A., Lerner, R. A., and Geysen, H. M. (1988) *Adv. Immunol. 43*, 1−98.
10. Arnon, R., and Van Regenmortel, M. H. V. (1992) *FASEB J. 6*, 3265−3274.
11. Nicholson, B. H. (1994) *Synthetic vaccines*, Blackwell Scientific Publications, Oxford, England.
12. Stanfield, L. R., Fieser, T. M., Lerner, R. A., and Wilson, I. A. (1990) *Science 248*, 712−719.
13. Wien, M. W., Filman, D. J., Stura, E. A., Guillot, S., Delpeyroux, F., Crainic, R., and Hogle, J. M. (1995) *Nat. Struct. Biol. 2*, 232−243.
14. Lescar, J., Stouracova, R., Riottot, M.-M., Chitarra, V., Brynda, J., Fabry, M., Horejsi, M., Sedlacek, J., and Bentley, G. A. (1997) *J. Mol. Biol. 267*, 1207−1222.
15. Molins, M. A., Contreras, M. A., Fita, I., and Pons, M. (1998) *J. Pept. Sci. 4*, 101−110.
16. Rini, J. M., Schulze-Gahmen, U., and Wilson, I. A. (1992) *Science 255*, 959−965.
17. Tsang, P., Rance, M., Fieser, T. M., Ostresh, J. M., Houghten, R. A., Lerner, R. A., and Wright, P. E. (1992) *Biochemistry 31*, 3862−3871.
18. Shoham, M. (1993) *J. Mol. Biol. 232*, 1169−1175.
19. Tormo, J., Blaas, D., Parry, N. R., Rowlands, D., Stuart, D., and Fita, I. (1994) *EMBO J. 13*, 2247−2256.
20. Davies, D. R., Sheriff, S., and Padlan, E. (1989) *Cold Spring Harbor Symp. Quant. Biol. 54*, 233−238.
21. Tulip, W. R., Varghese, J. N., Laver, W. G., Webster, R. G., and Colman, P. M. (1992) *J. Mol. Biol. 227*, 122−148.
22. Malby, R. L., Tulip, W. R., Harley, V. R., McKimm-Breschkin, J. L., Laver, W. G., Webster, R. G., and Colman, P. M. (1994) *Structure 15*, 733−746.
23. Bossart-Whitaker, P., Chang, C. Y., Novotny, J., Benjamin, D. C., and Sheriff, S. (1995) *J. Mol. Biol. 253*, 559−575.
24. Cohen, G. H., Sheriff, S., and Davies, D. R. (1996) *Acta Crystallogr. D52*, 315−326.
25. Scherf, T., Hiller, R., Naider, F., Levitt, M., and Anglister, J. (1992) *Biochemistry 31*, 6884−6897.
26. Dyson, H. J., and Wright, P. E. (1995) *FASEB J. 9*, 37−42.
27. Dyson, H. J., Cross, K. J., Houghten, R. A., Wilson, I. A., Wright, P. E., and Lerner, R. A. (1985) *Nature 318*, 480−483.
28. Dyson, H. J., Rance, M., Houghten, R. A., Lerner, R. A., and Wright, P. E. (1988) *J. Mol. Biol. 201*, 161−200.
29. Chandrasekhar, K., Profy, A. T., and Dyson, H. J. (1991) *Biochemistry 30*, 9187−9194.
30. Schulze-Gahmen, U., Rini, J. M., and Wilson, I. A. (1993) *J. Mol. Biol. 234*, 1098−1118.
31. Zvi, A., Feigelson, D. J., Hayek, Y., and Anglister, J. (1997) *Biochemistry 36*, 8619−8627.
32. Cheetham, J. C., Raleigh, D. P., Griest, R. E., Redfield, C., Dobson, C. M., and Rees, A. R. (1991) *Proc. Natl. Acad. Sci. U.S.A. 88*, 7968−7972.
33. Mani, J. C., Marchi, V., and Cucurou, C. (1994) *Mol. Immunol. 31*, 439−444.
34. Rondard, P., Brégégère, F., Lecroisey, A., Delepierre, M., and Bedouelle, H. (1997) *Biochemistry 36*, 8954−8961.
35. Foote, J., and Milstein, C. (1991) *Nature 352*, 530−532.
36. Foote, J., and Eisen, H. N. (1995) *Proc. Natl. Acad. Sci. U.S.A. 92*, 1254−1256.
37. Al Moudallal, Z., Briand, J. P., and Van Regenmortel, M. H. V. (1985) *EMBO J. 4*, 1231−1235.
38. Bloomer, A. C., Champness, J. A., Bricogne, G., Staden, R., and Klug, A. (1978) *Nature 276*, 362−368.
39. Mondragon, A. (1984) Ph.D. Thesis, University of Cambridge, U.K.
40. Chatellier, J., Rauffer-Bruyère, N., Van Regenmortel, M. H. V., Weiss, E., and Altschuh, D. (1996) *J. Mol. Recognit. 9*, 39−51.
41. Al Moudallal, Z., Briand, J. P., and Van Regenmortel, M. H. V. (1982) *EMBO J. 1*, 1005−1010.
42. Richalet-Sécordel, P. M., Rauffer-Bruyère, N., Christensen, L. L. H., Ofenloch-Haehnle, B., Seidel, C., and Van Regenmortel, M. H. V. (1997) *Anal. Biochem. 249*, 165−173.
43. Chatellier, J., Van Regenmortel, M. H. V., Vernet, T., and Altschuh, D. (1996) *J. Mol. Biol. 264*, 1−6.
44. Hwang, D.-J., Roberts, I. M., and Wilson, T. M. A. (1994) *Proc. Natl. Acad. Sci. U.S.A. 91*, 9067−9071.
45. Hochuli, E., BannWarth, W., Döbeli, H., Gentz, R., and Stüber, D. (1988) *Bio/Technology 6*, 1321−1325.
46. Zaitlin, M., and Ferris, W. R. (1964) *Science 143*, 1451−1452.
47. Kunkel, T. A. (1985) *Proc. Natl. Acad. Sci. U.S.A. 82*, 488−492.
48. Vieira, J., and Messing, J. (1987) *Methods Enzymol. 153*, 3−11.
49. Studier, F. W., Rosenberg, A. H., Dunn, J. J., and Dubendorff, J. W. (1990) *Methods Enzymol. 185*, 60−89.
50. Sambrook, J., Fritsch, E. F., and Maniatis, T. (1989) *Molecular cloning: A laboratory manual*, Cold Spring Harbor Laboratory Press, Cold Spring Harbor, NY.
51. Towbin, H., Staehelin, T., and Gordon, J. (1979) *Proc. Natl. Acad. Sci. U.S.A. 76*, 4350−4354.
52. Löfås, S., and Johnsson, B. (1990) *J. Chem. Soc., Chem. Commun. 21*, 1526−1528.
53. Christensen, L. H. (1997) *Anal. Biochem. 249*, 153−164.
54. Karlsson, R., Roos, H., Fägerstam, L., and Persson, B. (1994) *Methods: Comput. Methods Enzymol. 6*, 99−110.
55. O'Shannessy, D. J., Brigham-Burke, M., Soneson, K. K., Hensley, P., and Brooks, I. (1993) *Anal. Biochem. 212*, 457−468.
56. Roden, L. D., and Myszka, D. G. (1996) *Biochem. Biophys. Res. Commun. 225*, 1073−1077.
57. Karlsson, R., and Fält, A. (1997) *J. Immunol. Methods 200*, 121−133.
58. Saunal, H. (1995) Ph.D. Thesis, University Louis Pasteur, Strasbourg, France.
59. Saunal, H., Witz, J., and Van Regenmortel, M. H. V. (1993) *J. Gen. Virol. 74*, 897−900.
60. Lehrman, S. R., Tuls, J. L., and Lund, M. (1990) *Biochemistry 29*, 5590−5596.
61. Alexander, H., Alexander, S., Getzoff, E. D., Tainer, J. A., Geysen, H. M., and Lerner, R. A. (1992) *Proc. Natl. Acad. Sci. U.S.A. 89*, 3352−3356.
62. Rondard, P., and Bedouelle, H. (1999) *J. Biol. Chem.* (in press).
63. Burgen, A. S. V., Roberts, G. C. K., and Feeney, J. (1975) *Nature 253*, 753−755.
64. Malmqvist, M. (1994) *J. Mol. Recognit. 7*, 1−7.
65. Doyle, M. L., Myszka, D. G., and Chaiken, I. M. (1996) *J. Mol. Recognit. 9*, 65−74.

BI982011Z